Science Bulletin 64 (2019) 1049–1055

Contents lists available at ScienceDirect

Science Bulletin

journal homepage: www.elsevier.com/locate/scib

Science Bulletin
www.scibull.com

Article

A field-effect approach to directly profiling the localized states in monolayer MoS_2

Hao Wu [a,1], Yuan Liu [a,*,1], Zeyu Deng [b,1], Hung-Chieh Cheng [a], Dehui Li [b], Jian Guo [a], Qiyuan He [b], Sen Yang [a], Mengning Ding [a], Yun-Chiao Huang [a], Chen Wang [a], Yu Huang [a,c], Xiangfeng Duan [b,c,*]

[a] Department of Materials Science and Engineering, University of California, Los Angeles, CA 90095, USA
[b] Department of Chemistry and Biochemistry, University of California, Los Angeles, CA 90095, USA
[c] California NanoSystems Institute, University of California, Los Angeles, CA 90095, USA

ARTICLE INFO

Article history:
Received 21 February 2019
Received in revised form 8 April 2019
Accepted 14 May 2019
Available online 23 May 2019

Keywords:
Two-dimensional layered materials
Field-effect transistor
Localized states
Electronic transport
Conductivity plateau

ABSTRACT

A fundamental understanding of the charge transport mechanism in two-dimensional semiconductors (e.g., MoS_2) is crucial for fully exploring their potential in electronic and optoelectronic devices. By using monolayer graphene as the barrier-free contact to MoS_2, we show that the field-modulated conductivity can be used to probe the electronic structure of the localized states. A series of regularly distributed plateaus were observed in the gate-dependent transfer curves. Calculations based on the variable-range hopping theory indicate that such plateaus can be attributed to the discrete localized states near mobility edge. This method provides an effective approach to directly profiling the localized states in conduction channel with an ultrahigh resolution up to 1 meV.

1. Introduction

Two-dimensional layered materials (2DLMs) represent an exciting class of materials with intriguing properties such as metal-insulator transition [1], superconductivity [2], and Shubnikov-de Haas oscillations [3]. Among these materials, molybdenum disulfide (MoS_2) is the most investigated n-type semiconductor with a direct bandgap of 1.8 eV for monolayers and an indirect bandgap of 1.2 eV for multilayers [4–6]. The atomically thin geometry of 2D semiconductors may promise lower power dissipation electronic devices [7–13], and have also generated considerable interest for diverse optoelectronic applications [14–18]. However, the attained experimental field-effect mobility of MoS_2 supported on SiO_2 substrate is still considerably lower than the theoretical value [1,19–21], which is largely attributed to the scattering by disorders [22–24].

Recent studies have demonstrated that encapsulation of MoS_2 in the high-k dielectrics and passivation by the boron nitride could suppress the disorders, therefore leading to high mobility [1,3,20]. Additionally, the suppression of disorders contributes to a transition into metallic states at a lower carrier concentration [19]. In the metallic regime, the electronic transport is mainly dominated by the extended states. But in the insulating regime, the electronic transport shows the characteristics of variable-range hopping (VRH) at cryogenic temperature, indicating the presence of localized states [25–27]. Recent studies suggest that the structural disorders are the primary sources of localized states while the charge trap at the SiO_2/MoS_2 interface also contributes [19]. Transmission electron microscopy (TEM) [28], scanning tunneling microscopy (STM) [29] and the capacitance measurements [30,31] have been utilized to investigate the localized states with their own merits and drawbacks. For instance, it is impossible to obtain the electronic structure of localized states with TEM, while the STM is merely able to resolve the electronic structure on the upper surface of MoS_2. Capacitance measurement can resolve the density of states (DOS) of localized states, but it is incapable of excluding the capacitance of the localized states away from the multilayer MoS_2/SiO_2 interface. Moreover, the localized states capacitance is rather small compared to the total capacitance, thus greatly degrading the DOS resolution [31]. Overall, these techniques are insufficient to offer direct information on the conduction along the interface [29–31], which is important for the charge transport behavior and potential applications of atomically thin MoS_2.

SPECIAL TOPIC: Two-dimensional Materials: New Opportunities for Electronics, Photonics and Optoelectronics

* Corresponding authors.
E-mail addresses: yuanliuhnu@hnu.edu.cn (Y. Liu), xduan@chem.ucla.edu (X. Duan).

[1] These authors contributed equally to this work.

https://doi.org/10.1016/j.scib.2019.05.021
2095-9273/

Here we report a field-effect approach to directly probe the localized states in monolayer MoS_2. Distinct from the previous indirect studies, the field-effect transport offers a robust approach to tune the carrier concentration and unambiguously probe the electronic states in conduction channel of MoS_2. By applying a gate voltage, the Fermi level can be readily tuned throughout the bandgap of MoS_2, thus the transport properties of each state in the vicinity of the Fermi level can be probed. Furthermore, this method can effectively avoid altering the intrinsic properties of MoS_2. For 2D electron gas systems, such technique has been widely utilized to study their transport phase diagram [32]. Particularly, Marré and co-workers [33] have studied the localized states at the interface of $LaAlO_3/SrTiO_3$ and observed thermal power oscillation with varying gate voltage, which is attributed to multiple discrete localized states. Nonetheless, Marré's study was unable to observe the theoretically predicated periodic conductivity plateaus due to the non-Ohmic contacts.

In this research, we for first time discovered the conductivity plateaus induced by the localized states of MoS_2 without magnetic field. Distinct from the conventional MoS_2 field effect transistor (FET) with metal contacts, the MoS_2 samples are contacted with monolayer graphene as electrodes, enabling barrier-free contacts and direct probing the localized states with small excitation voltage ($V_{ds} \leq 0.5$ mV). By combining the experiments and algorithms based on VRH model, we achieve a very high resolution (up to 1 meV) profiling localized states in MoS_2. The findings provide important insights into the fundamental transport properties of MoS_2 and potentially offer the strategy to improve the performances of MoS_2 devices.

2. Device fabrication

To investigate the transport properties of MoS_2, field effect transistors (FET) were constructed on a 300 nm SiO_2/Si substrate using monolayer MoS_2 as the semiconducting channel and two strips of monolayer graphene underneath the MoS_2 as the source/drain electrodes (Fig. 1a, inset of Fig. 1b). The graphene contact to MoS_2 has been demonstrated as a barrier-free transparent contact [20]. The transistors were measured in dark from 1.9 to 300 K. The monolayer MoS_2 FETs show perfect linear current-voltage (I_{ds}-V_{ds}) behavior with different gate voltages at 1.9 K (Fig. 1b), suggesting Ohmic contacts, which are further confirmed by the positive slope in Arrhenius plot (Fig. S1 online) [20,34].

3. Results

3.1. Device measurements

Fig. 2a illustrates the gate voltage dependence of MoS_2 sheet conductivity measured up to back gate voltage $V_{bg} = 80$ V at various temperatures. The use of back gate allows effective tuning of accumulated carrier concentration up to $4.72 \times 10^{12}/cm^2$ with applied gate voltage up to 60 V at room temperature, according to gate capacitance model $n = C_{ox}(V_{bg} - V_{th})$ [35], where n is the accumulated carrier concentration, C_{ox} is 12 nF/cm^2 for the capacitance of 300 nm SiO_2, V_{bg} is the gate voltage, and V_{th} is the threshold gate voltage. In the high carrier concentration regime (V_{bg}> 60 V), the sheet conductivity increases with decreasing temperature, suggesting a metallic behavior of MoS_2. This metallic behavior is related to the interplay of the electron-electron interaction and the disorders [26,32,36]. In the metallic regime, the disorders are suppressed and the metallic state can be stabilized by the Coulomb interaction between electrons. When the gate voltage is below a critical value (V_{bg} < 40 V), the conductivity decreases with decreasing temperature in range of 210 and 1.9 K, indicating a typical semiconductor behavior which is also conventionally referred as "insulating state". The conductivity divergent point between metallic state and insulating state ($\sim e^2/h$) [1], was also observed. In the insulating regime, the disorders, including extrinsic charge impurities at the MoS_2/SiO_2 interface and the intrinsic defects such as sulfur vacancies, prevail and dominate the electron transport at low temperatures [22].

The existence of the disorders can also be proved by the temperature dependence of mobility. Fig. 2b shows the mobility as a function of gate voltage and temperature. The field-effect mobility is evaluated by $\mu = dI_{ds}/dV_{dg} \times (L/W)/(C_{ox} \times V_{ds})$, where L is the channel length and W is the channel width. Above 90 K, the mobility at all gate voltages keeps increasing with lowering temperature and can be fitted using $\mu \sim T^{-v}$, where $v \approx 0.49 \sim 0.76$, which is in agreement with previous studies of phonon scattering governed transport in 2D electron systems [21,37–39]. The phonon scattering is expected to be suppressed in the cryogenic regime, where the dominant scattering mechanisms are long-range charged impurity scattering and short-range neutral impurity scattering. Indeed, the mobility at a lower gate voltage (V_{bg} < 30 V) decreases with decreasing temperature from 90 to 1.9 K (Fig. 2b). This drop indicates that the impurity scattering begins to play a more

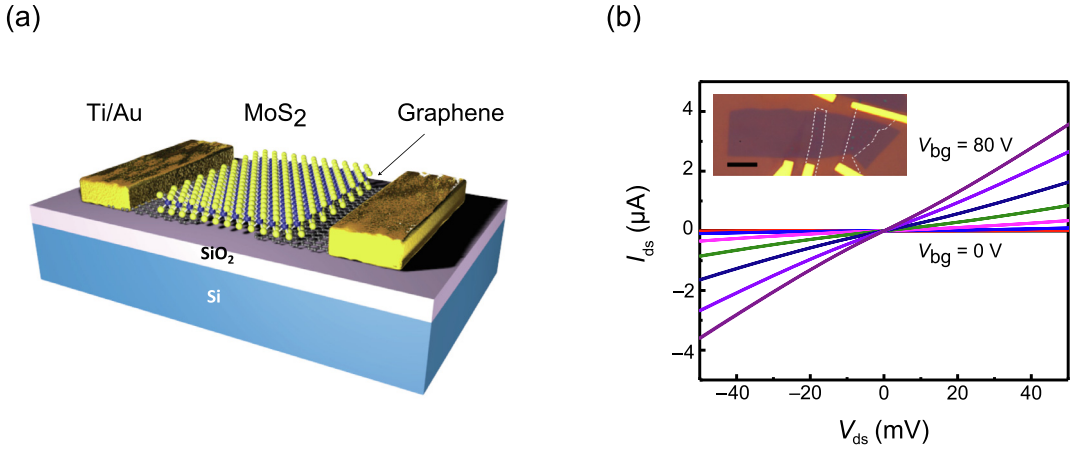

Fig. 1. (Color online) The schematic and the I_{ds}-V_{ds} output of monolayer MoS_2 device at 1.9 K. (a) Schematic of a monolayer MoS_2 FET with monolayer graphene contacts. The drain and source graphene contacts are connected to Ti/Au (50 nm/50 nm) electrodes. (b) The I_{ds}-V_{ds} curves of MoS_2 FET with different back gate voltage V_{bg} at 1.9 K. The inset shows an optical image of a monolayer MoS_2 device. The graphene electrodes are marked by dashed lines. Scale bar, 5 μm.

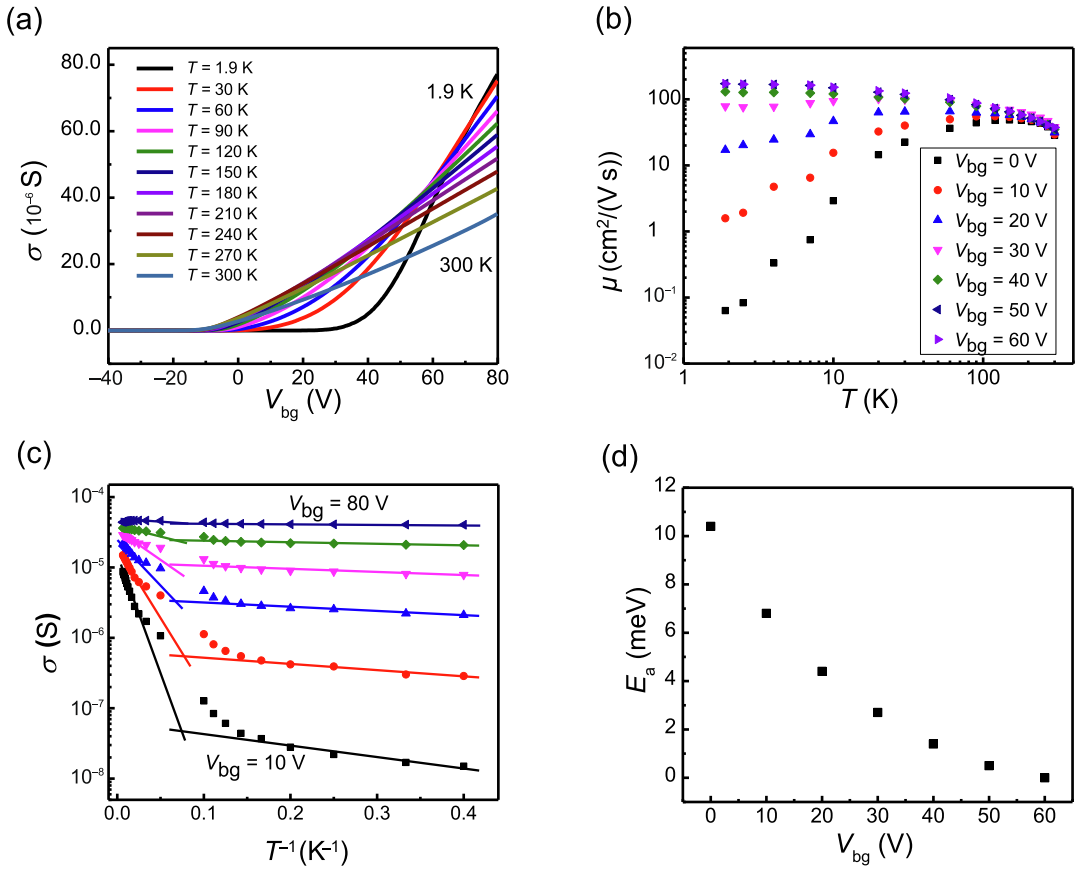

Fig. 2. (Color online) Transfer curves and temperature-dependent transport properties of MoS_2 FET. (a) The transfer curves of MoS_2 FET from 300 to 1.9 K. (b) The mobility of MoS_2 as a function of temperature at different gate voltages from 0 to 60 V. (c) The Arrhenius plot of the sheet conductivity σ of monolayer MoS_2 in the insulating regime (V_{bg} < 60 V). (d) The activation energy E_a as a function of V_{bg}.

important role at low temperature [1,40]. However, the mobility at a higher gate voltage (V_{bg} > 30 V) does not exhibit the similar trend below 90 K. Instead, it keeps increasing and finally saturates as the temperature approaches 1.9 K. The absence of the mobility decline with decreasing temperature is attributed to the more efficient screening of Coulomb scattering with larger carrier concentration [40].

Fig. 2b also reveals that the mobility exhibits saturation with increasing gate voltage, which is consistent with previous reports [3,22]. In the cryogenic temperature regime (1.9 K < T < 90 K), the screening of long-range Coulomb scattering leads to the enhancement of mobility when V_{bg} < 30 V. When V_{bg} > 30 V, the long-range Coulomb scattering is gradually eliminated and leaving carrier concentration-independent short-range scattering as the primary mobility limiting factor, which has been well-studied in graphene [41]. When T > 90 K, a similar mobility saturation at high gate voltage is also observed. With higher V_{bg}, the enhanced screening of impurity scattering increases the mobility. Meanwhile, phonon-electron scattering also increases because of stronger Fröhlich interaction [42–44].

3.2. Carrier transport

To gain a further insight into the transport, the Arrhenius plot of sheet conductivity obtained at V_{ds} = 0.1 V is shown in Fig. 2c. In the high temperature regime (T > 30 K), the sheet conductivity σ of MoS_2 can be described as thermal-activated transport [1]. In this band-like transport, carriers are thermally activated to the delocalized extended states above the mobility edge and can be freely driven by the electric field. Therefore, the sheet conductivity depends mainly on the carrier concentration at extended states and can be fitted with $\sigma = \sigma_0 \exp(-E_a/kT)$, where σ_0 is the prefactor of sheet conductivity, E_a is the thermal activation energy. Using this equation, E_a is found to decrease with increasing carrier concentration because the Fermi level is moving closer to the mobility edge [45]. As shown in the Fig. 2d, with higher V_{bg}, E_a keeps decreasing from 10.4 to 0 mV, indicating electrons becomes more delocalized, consistent with the percolation model [31].

Upon further decreasing temperature below 30 K, the thermal activation of electron is barely possible and electrons mostly occupy the localized states below the mobility edge rather than the extended states above the mobility edge. Therefore, the dependence of sheet conductivity on the temperature is weakened. The dominating transport behavior in this regime is attributed to the VRH and can be described as $\sigma = \sigma_0 \exp[-(T_0/T)^{1/(d+1)}]$, where σ_0 is the sheet conductivity prefactor, T_0 is the correlation energy scale, T is the temperature and d is the dimension of the system [23,25,46]. Previous study suggests that the VRH at low temperature originates from the midgap intrinsic defect states in the MoS_2 samples and trap states at the MoS_2/SiO_2 interface [19].

3.3. Conductivity plateaus

To further examine the localized states in MoS_2, small bias voltage on the order of 0.1 mV was applied. Distinct from the 0.1 V bias voltage applied in Fig. 2a, a small bias would not excite the electrons to the extended states above the mobility edge, therefore the electrons migrate at the states near the Fermi level. Fig. 3a

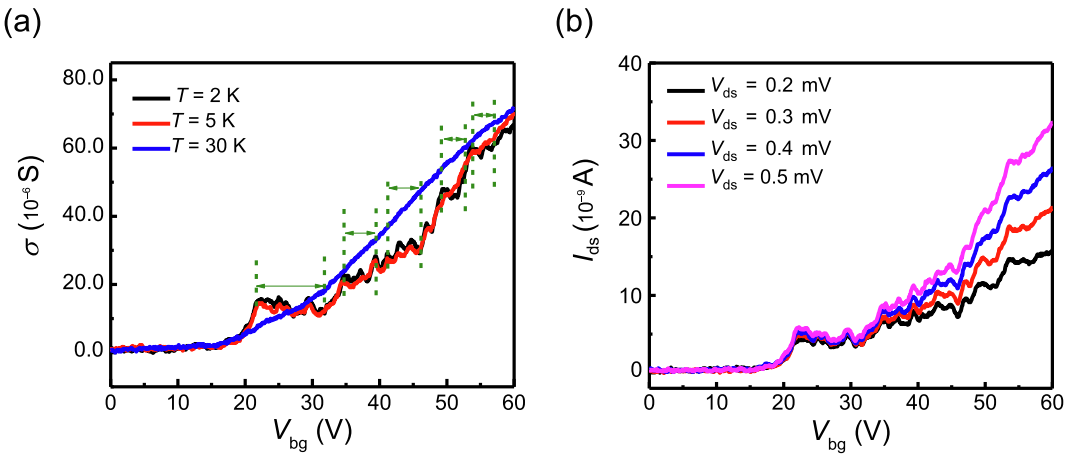

Fig. 3. (Color online) The temperature-dependent and bias voltage-independent sheet conductivity plateaus. (a) The sheet conductivity σ as a function of V_{bg} at 2, 5, and 30 K with V_{ds} = 0.5 mV. The dashed lines indicate the width of the conductivity plateaus. The conductivity plateaus can be clearly observed in the 2 K curves and gradually disappear when temperature increases. (b) The current plateaus at 5 K with different V_{ds}.

shows the transfer curves with V_{ds} = 0.5 mV respectively at 2, 5, and 30 K. Importantly, these transfer curves show dramatically different features from those at high bias voltage (V_{ds} = 0.1 V) with notable conductivity plateaus. Several conductivity plateaus, marked with dashed lines, can be observed in the transfer curves of Fig. 3a. The plateau at lowest gate voltage spans from 22 to 32 V along the V_{bg}-axis, but as V_{bg} increases, the width of conductivity plateau gradually reduces to 5 V. Besides, the plateaus are reproducible and robust when the V_{bg} is measured back and forth (Fig. S2 online). Additionally, the universal conductance fluctuation (UCF) patterns are also found to superimpose those plateaus. In contrast to the wide conductivity plateaus, the universal conductance fluctuation patterns are a set of randomly distributed peaks with full width at half maximum around 1 V. The signatures of the universal conductance fluctuation are consistent with those found in other 2D electron gas systems with disorders, such as Si and graphene [47,48].

When the temperature is above 5 K, the UCF patterns almost vanish while the conductivity plateaus still exist. When the temperature further rises to 30 K, the conductivity plateaus disappear as well. The reasons for divergent characteristics of two patterns lie in the different nature of the two transport processes. UCF is a coherent transport that is more sensitive to temperature than the phonon assisted hopping. Typically, UCF requires a large resonant density of states to be built up, whose process usually takes ~0.01 s in a 2D electron gas system, without destructively incoherent scattering [48,49]. Nevertheless, the hopping is a diffusive transport. Therefore, the disappearance of plateaus is caused by thermal broadening of carrier distribution near the Fermi level. Fig. 3b illustrates the transfer curve at 5 K with different bias voltages and the positions of plateaus are independent of bias voltage. As the bias voltage determines the electrons momentum, the plateaus positions are supposed to shift with different bias voltages if the transport was coherent [50]. In contrast, the independence of plateau with bias voltage in our measurements indicates that the transport is dominated by the incoherent hopping process, where different conductive paths do not interfere.

4. Discussion and conclusions

We have qualitatively investigated the localized-state induced conductivity plateaus, which are observed for the first time in the 2D systems as far as we know. We attribute this discovery to the barrier-free graphene contact. The existence of Schottky barrier in conventional MoS_2 FETs requires a large bias voltage to turn on the devices. When the excitation voltage exceeds a certain value, the carrier would be pumped to the extended states, making the localized electrons transport less significant. Another reason is that the voltage excitation also broadens the conduction energy level in the same mechanism as temperature does [51]. Thus, when the bandwidth of conduction energy level exceeds that of discrete localized states, the signatures would disappear. In order to elucidate the effect of the contact on the observation of conductivity plateaus, MoS_2 FETs with 5 nm/50 nm Cr/Au contacts were also fabricated. In a negligible number of devices with undetectable Schottky barrier through the Arrhenius plot method, the similar behavior was also observed (Fig. S3 online). However, most devices exhibit imperfect contacts with no conductivity plateaus observed, confirming the indispensable role of barrier-free contact.

4.1. Simulations

To confirm the hypothesis of plateaus' origin, the sheet conductivity of MoS_2 was simulated quantitatively using a VRH model including a series of discrete localized states. This model can reproduce the conductivity plateaus and the plateau evolution as a function of temperature. Two types of states, the localized states and extended states, are included in this model and the mobility edge acts as the boundary separating those two kinds of states. Below the mobility edge, the electrons hop to the most probable localized states with the assistance of a phonon; while for the transport of extended states above the mobility edge, the electrons behave as free electrons in a band-like transport. Therefore, the transport in this model is a combination of two mechanisms, which have been proved before [30]. For the electrons in the extended states, the theoretical band mobility was used [43]. In addition, as previously described, the positions of localized states in the band diagram were estimated by the activation energy fitted from the experimental data in the thermal transport regime (T > 30 K) with $\sigma = \sigma_0 \exp(-E_a/kT)$.

The net hopping conductivity can be calculated by the integration of the differential sheet conductivity of each states contributing to the conduction [52]. Furthermore, the differential sheet conductivity is a complicated function of the distribution of localized states. Therefore, the distribution of localized states can be obtained. Specifically, the DOS of the localized states were calculated by minimizing the deviation between theoretical and

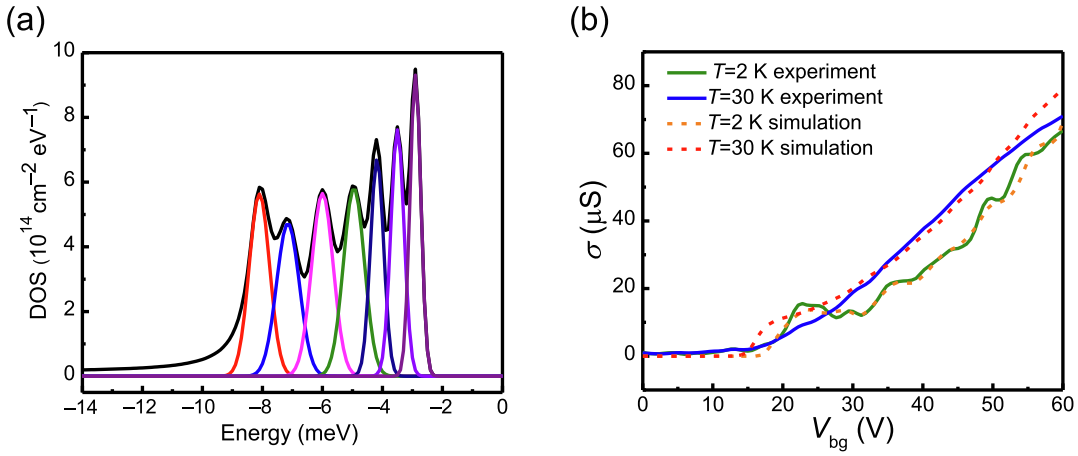

Fig. 4. (Color online) Simulation of localized states and MoS_2 FET transfer curves. (a) The DOS of localized states obtained with VRH model. 0 meV is the mobility edge. (b) The simulated transfer curves at 2 and 30 K with the localized states in Fig. 4a and the corresponding experimental transfer curves.

experimental transfer curves below 30 K. The profile of the discrete localized states was shown in the Fig. 4a. The mobility edge is 0 meV in this diagram and the localized states are distributed in the range of −12 to −2 meV, which is close to the range estimated from the experiment (Fig. 2d). Additionally, by integrating the DOS, the total concentration of localized states is estimated to be 4.52×10^{12}/cm^2, consistent with the concentration of atomic defects in previous TEM study [28]. It indicates that the localized states are normally resulted from the intrinsic surface states or fabrication induced defects states. At last, we would like to note that the profile of those localized states is enveloped in an exponential decaying function that was widely used to describe the localized states distribution [30]. Together with this approach, the precision of electronic structure can be pushed up to the limit of 1 meV.

The simulated transfer curves at 2 and 30 K are illustrated in Fig. 4b. The key features in the experimental data are reproduced in the simulated curves. In the experiments, the width of conductivity plateau observed becomes narrower with higher gate voltage. In our model, the reason is that the uplifted Fermi level would be closer to the mobility edge with higher V_{bg}, making more electrons occupy the extended states. Therefore, the growing number of delocalized electrons covers up the features of VRH. Additionally, the disappearance of plateau at higher temperature can also be interpreted. The bandwidth of conduction energy level approximately equals to $4kT$ [53,54]. Once the width of conduction energy level exceeds that of a localized state as temperature increases, the corresponding plateau would vanish as the results of "thermal smearing". In our case, the width of localized states is approximately 2 mV. Hence as the temperature reaches 6 K, the conduction energy level starts to "smear" the adjacent localized states. Therefore, the adjacent localized states near the Fermi level contribute to the conduction and become irresolvable, making the plateaus vanish. When the temperature exceeds 30 K, the conduction energy level is wider than that of the localized states region, leading to the complete disappearance of conduction plateaus.

To further verify that the conductive plateaus are induced by the localized states, a multilayer MoS_2 device was also measured and simulated with the same procedures (Figs. S4–S6 online). The simulation results confirm the DOS of localized states in monolayer MoS_2 is higher than that in multilayer MoS_2, suggesting the monolayer MoS_2 is a more disordered system. This trend is consistent with capacitance measurements [31].

4.2. Conclusions

In conclusion, we have measured the transport properties of MoS_2 with graphene as barrier-free contacts. The sheet conductivity and mobility versus temperature relationships reveal that the VRH dominates the transport property below 30 K. In the hopping transport dominated temperature range, the transfer curves with low bias voltage ($V_{ds} \leq 0.5$ mV) display a series of conductivity plateaus, which are induced by the discrete localized states in the MoS_2.

This behaviour was unprecedented in the previous literatures due to the non-Ohmic contact to the MoS_2. With graphene contacts, we firstly observed this behaviour and the electronic structure of the localized states can be resolved within the framework of VRH model. The electronic structure of localized states is directly characterized and the resolution of the localized states can be achieved up to 1 meV, which is beyond the limit of the conventional techniques. In this regard, our method offers a general approach for directly probing the localized states and a direct evidence of the hopping transport origin.

Conflict of interest

The authors declare that they have no conflict of interest.

Acknowledgments

X.D. acknowledges the support by the National Science Foundation (DMR1508144). Y. H. acknowledges the financial support from the National Science Foundation (EFRI-1433541).

Author contributions

Hao Wu and Yuan Liu designed the experiments and simulations. Hao Wu, Zeyu Deng, and Dehui Li implemented the simulation software and algorithm. Hung-Chieh Cheng, Yuan Liu, Jian Guo, and Qiyuan He got involved in the device fabrication. Yuan Liu, Dehui Li, and Hao Wu contribute to the cryogenic measurement system setup and related measurement software implementation. Sen Yang, Mengning Ding, Yun-Chiao Huang and Chen Wang contributed to the device characterizations. All authors contributed to the interpretation and discussion of the results.

Appendix A. Supplementary data

Supplementary data to this article can be found online at https://doi.org/10.1016/j.scib.2019.05.021.

References

[1] Radisavljevic B, Kis A. Mobility engineering and a metal-insulator transition in monolayer MoS_2. Nat Mater 2013;12:815–20.
[2] Ye JT, Zhang YJ, Akashi R, et al. Superconducting dome in a gate-tuned band insulator. Science 2012;338:1193–6.
[3] Cui X, Lee GH, Kim YD, et al. Multi-terminal transport measurements of MoS_2 using a van der Waals heterostructure device platform. Nat Nanotechnol 2015;10:534–40.
[4] Mak KF, Lee C, Hone J, et al. Atomically thin MoS_2: a new direct-gap semiconductor. Phys Rev Lett 2010;105:136805.
[5] Splendiani A, Sun L, Zhang YB, et al. Emerging photoluminescence in monolayer MoS_2. Nano Lett 2010;10:1271–5.
[6] Kam KK, Parkinson BA. Detailed photocurrent spectroscopy of the semiconducting group-vi transition-metal dichalcogenides. J Phys Chem 1982;86:463–7.
[7] Sarkar D, Xie XJ, Liu W, et al. A subthermionic tunnel field-effect transistor with an atomically thin channel. Nature 2015;526:91–5.
[8] Yap WC, Yang Z, Mehboudi M, et al. Layered material GeSe and vertical GeSe/MoS_2 p-n heterojunctions. Nano Res 2018;11:420–30.
[9] Cheng R, Jiang S, Chen Y, et al. Few-layer molybdenum disulfide transistors and circuits for high-speed flexible electronics. Nat Commun 2014;5:5143.
[10] Liu Y, Guo J, Zhu E, et al. Approaching Schottky-Mott limit in van der Waals metal-semiconductor contacts. Nature 2018;557:696–700.
[11] Liu Y, Guo J, Wu Y, et al. Pushing the performance limit of sub-100 nm molybdenum disulfide transistors. Nano Lett 2016;16:6337–42.
[12] Liu Y, Duan X, Huang Y, et al. Two-dimensional transistors beyond graphene and TMDCs. Chem Soc Rev 2018;47:6388–409.
[13] Liu Y, Huang Y, Duan XF. Van der Waals integration before and beyond two-dimensional materials. Nature 2019;567:323–33.
[14] Mak KF, McGill KL, Park J, et al. The valley Hall effect in MoS_2 transistors. Science 2014;344:1489–92.
[15] Amani M, Lien DH, Kiriya D, et al. Near-unity photoluminescence quantum yield in MoS_2. Science 2015;350:1065–8.
[16] Tian H, Chin ML, Najmaei S, et al. Optoelectronic devices based on two-dimensional transition metal dichalcogenides. Nano Res 2016;9:1543–60.
[17] Yu WJ, Vu QA, Oh H, et al. Unusually efficient photocurrent extraction in monolayer van der Waals heterostructure by tunnelling through discretized barriers. Nat Commun 2016;7:13278.
[18] Wan X, Chen K, Chen ZF, et al. Controlled electrochemical deposition of large-area MoS_2 on graphene for high-responsivity photodetectors. Adv Funct Mater 2017;27:1603998.
[19] Yu ZH, Pan YM, Shen YT, et al. Towards intrinsic charge transport in monolayer molybdenum disulfide by defect and interface engineering. Nat Commun 2014;5:5290.
[20] Liu Y, Wu H, Cheng HC, et al. Toward barrier free contact to molybdenum disulfide using graphene electrodes. Nano Lett 2015;15:3030–4.
[21] Kaasbjerg K, Thygesen KS, Jacobsen KW. Phonon-limited mobility in n-type single-layer MoS_2 from first principles. Phys Rev B 2012;85:115317.
[22] Li SL, Wakabayashi K, Xu Y, et al. Thickness-dependent interfacial coulomb scattering in atomically thin field-effect transistors. Nano Lett 2013;13:3546–52.
[23] Qiu H, Xu T, Wang ZL, et al. Hopping transport through defect-induced localized states in molybdenum disulphide. Nat Commun 2013;4:2642.
[24] Yu ZH, Ong ZY, Li SL, et al. Analyzing the carrier mobility in transition-metal dichalcogenide MoS_2 field-effect transistors. Adv Funct Mater 2017;27:1604093.
[25] Ghatak S, Pal AN, Ghosh A. Nature of electronic states in atomically thin MoS_2 field-effect transistors. ACS Nano 2011;5:7707–12.
[26] Hippalgaonkar K, Wang Y, Ye Y, et al. High thermoelectric power factor in two-dimensional crystals of MoS_2. Phys Rev B 2017;95:115047.
[27] Tran S, Yang JW, Gillgren N, et al. Surface transport and quantum Hall effect in ambipolar black phosphorus double quantum wells. Sci Adv 2017;3:e1603179.
[28] Hong JH, Hu ZX, Probert M, et al. Exploring atomic defects in molybdenum disulphide monolayers. Nat Commun 2015;6:6293.
[29] Lu CP, Li GH, Mao JH, et al. Bandgap, mid-gap states, and gating effects in MoS_2. Nano Lett 2014;14:4628–33.
[30] Zhu WJ, Low T, Lee YH, et al. Electronic transport and device prospects of monolayer molybdenum disulphide grown by chemical vapour deposition. Nat Commun 2014;5:3087.
[31] Chen XL, Wu ZF, Xu SG, et al. Probing the electron states and metal-insulator transition mechanisms in molybdenum disulphide vertical heterostructures. Nat Commun 2015;6:6088.
[32] Abrahams E, Kravchenko SV, Sarachik MP. Colloquium: metallic behavior and related phenomena in two dimensions. Rev Mod Phys 2001;73:251–66.
[33] Pallecchi I, Telesio F, Li DF, et al. Giant oscillating thermopower at oxide interfaces. Nat Commun 2015;6:6678.
[34] Das S, Chen HY, Penumatcha AV, et al. High performance multilayer MoS_2 transistors with scandium contacts. Nano Lett 2013;13:100–5.
[35] Zhang Y, Tan YW, Stormer HL, et al. Experimental observation of the quantum Hall effect and Berry's phase in graphene. Nature 2005;438:201–4.
[36] Punnoose A, Finkel'stein, AM.. Metal-insulator transition in disordered two-dimensional electron systems. Science 2005;310:289–91.
[37] Baugher BWH, Churchill HOH, Yang YF, et al. Intrinsic electronic transport properties of high-quality monolayer and bilayer MoS_2. Nano Lett 2013;13:4212–6.
[38] Chen JH, Jang C, Xiao SD, et al. Intrinsic and extrinsic performance limits of graphene devices on SiO_2. Nat Nanotechnol 2008;3:206–9.
[39] Steinberg H, Gardner DR, Lee YS, et al. Surface state transport and ambipolar electric field effect in Bi_2Se_3 nanodevices. Nano Lett 2010;10:5032–6.
[40] Schmidt H, Wang SF, Chu LQ, et al. Transport properties of monolayer MoS_2 grown by chemical vapor deposition. Nano Lett 2014;14:1909–13.
[41] Das Sarma S, Adam S, Hwang EH, et al. Electronic transport in two-dimensional graphene. Rev Mod Phys 2011;83:407–70.
[42] Yoon Y, Ganapathi K, Salahuddin S. How good can monolayer MoS_2 transistors be? Nano Lett 2011;11:3768–73.
[43] Kim S, Konar A, Hwang WS, et al. High-mobility and low-power thin-film transistors based on multilayer MoS_2 crystals. Nat Commun 2012;3:1011.
[44] Gelmont BL, Shur M, Stroscio M. Polar optical-phonon scattering in three and two dimensional electron gases. J Appl Phys 1995;77:657–60.
[45] Jariwala D, Sangwan VK, Late DJ, et al. Band-like transport in high mobility unencapsulated single-layer MoS_2 transistors. Appl Phys Lett 2013;102:173107.
[46] Wu J, Schmidt H, Amara KK, et al. Large thermoelectricity via variable range hopping in chemical vapor deposition grown single-layer MoS_2. Nano Lett 2014;14:2730–4.
[47] Fowler AB, Timp GL, Wainer JJ, et al. Observation of resonant tunneling in silicon inversion-layers. Phys Rev Lett 1986;57:138–41.
[48] Guimaraes MHD, Zomer PJ, Vera-Marun IJ, et al. Spin-dependent quantum interference in nonlocal graphene spin valves. Nano Lett 2014;14:2952–6.
[49] Stone AD, Lee PA. Effect of inelastic processes on resonant tunneling in one dimension. Phys Rev Lett 1985;54:1196–9.
[50] Liang WJ, Bockrath M, Bozovic D, et al. Fabry-Perot interference in a nanotube electron waveguide. Nature 2001;411:665–9.
[51] Mucciolo ER, Neto AHC, Lewenkopf CH. Conductance quantization and transport gaps in disordered graphene nanoribbons. Phy Rev B 2009;79:075407.
[52] Nagy A, Hundhausen M, Ley L, et al. Steady-state hopping conduction in the conduction-band tail of a-Si-H studied in thin-film transistors. Phys Rev B 1995;52:11289–95.
[53] Lin YM, Perebeinos V, Chen ZH, et al. Electrical observation of subband formation in graphene nanoribbons. Phys Rev B 2008;78:161409.
[54] Seibel C, Nuber A, Bentmann H, et al. Quantized electronic fine structure with large anisotropy in ferromagnetic Fe films. Phys Rev B 2014;90:035136.

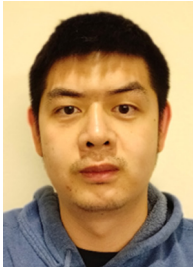

Hao Wu is currently a Senior Software Engineer and Project Lead at ASML. He graduated from University of California, Los Angeles in 2017 with a Ph.D. degree in Materials Engineering. Prior to that, he received his B.S. degree in Physics from Nankai University in 2011. His research interests include novel electronic device architecture design, charge transport simulation, and scalable software development leveraging distributed computing technique.

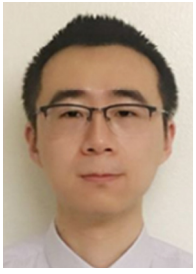

Yuan Liu is a Professor at the School of Physics and Electronics, Hunan University. He received his B.S. degree from the Zhejiang University in 2010, and Ph.D. degree from University of California, Los Angles in 2015. He was previously postdoc researcher in University of California, Los Angeles before joining Hunan University. His current research interests include novel electronics and optoelectronics based on new semiconductor materials and new device structure.

Zeyu Deng received the degree of Bachelor of Microelectronic Science and Engineering at Tsinghua University in 2017. Now he is seeking the Ph.D. degree in Electrical and Computer Engineering at University of California, Santa Barbara. He previously worked as an undergraduate research assistant at University of California, Los Angles under supervision of Prof. Xiangfeng Duan. His research covers transport properties of electrical devices, signal compression and coding theory.

Xiangfeng Duan is a Professor of Chemistry and Nanoscience at University of California, Los Angels. He received his B.S. degree from the University of Science and Technology of China in 1997, and Ph.D. degree from Harvard University in 2002. He was previously a Founding Scientist and then Manager of Advanced Technology at Nanosys Inc., a nanotechnology startup founded based partly on his doctoral research. His research interests include nanoscale materials and devices and their applications in future electronic, energy and health technologies.